Synthesis of Porous Carbon Hollow Particles Maintaining Their Structure using Hyper-Cross-Linked Poly(St-DVB) Hollow Particles

AUTHOR NAMES. Yusuke Kawai, Tetsuya Yamamoto*

AUTHOR ADDRESS. Department of Materials Design Innovation Engineering, Nagoya University, Furo-cho, Chikusa-ku, Nagoya, 464-8603, Japan

AUTHOR EMAIL ADDRESS. yamamoto.tetsuya@material.nagoya-u.ac.jp

CORRESPONDING AUTHOR FOOTNOTE. Phone: +81-52-789-3378, Fax: +81-52-789-3271,

E-mail: yamamoto.tetsuya@material.nagoya-u.ac.jp

Abstract

Porous carbon hollow particles (PCHPs) have many useful features such as a high specific surface area, large pore volume, and the presence of nanovoids, giving them potential for use in catalyst carriers, supercapacitors, and Li-ion batteries. However, conventional synthesis methods have many problems. In this study, we developed a new method to produce hollow polymer particles that retain their structure after carbonization, without using any templates which need to be removed later. These poly(styrene-divinylbenzene) (Poly(St-DVB)) hollow particles are hyper-cross-linked by Friedel-Crafts alkylation, which prevents collapse during carbonization. The synthesized PCHPs have a large specific surface area, and abundant micropores and macropores derived from their hollow structure. The shell of the PCHPs was found to be composed of amorphous carbon partially crystallized as graphite.

Keyword: Carbon hollow particles, Polystyrene, Hyper-cross-linking, Carbonization

1. Introduction

Porous carbon hollow particles (PCHPs) have many attractive features, such as large specific surface area, large pore volume, great thermal and chemical stability, good electrical conductivity, effective electromagnetic wave absorption, rapid diffusion of materials inside the shell, and the presence of nanovoids. These appealing characteristics have captivated many researchers around the world, and significant research is being carried out to find applications for PCHPs in catalyst carriers, supercapacitors, Li-ion batteries, and adsorption sensor technologies [1-7].

Hard templating is the most common way to synthesize PCHPs, but this method has some serious problems. It is implemented by: 1) synthesis of hard templates using silica or other hard materials, 2) coating of a carbon source, 3) removal of the templates, 4) carbonization [3]. This method enables fine control of the particle diameter and void size [8]. On the other hand, template removal requires the use of highly corrosive chemicals such as hydrofluoric acid, which is a problem from the viewpoint of safety, processing cost, and environmental protection [6, 9]. In addition, the necessity for complex and time-consuming surface modification when coating the carbon source [3, 10], and serious collapse of the hollow structure during template removal are also issues which must be resolved. In order to solve these problems, micelle, block copolymer,

bubble, and organic framework methods which do not require templates to be removed have been reported [6, 11-13]. However, because of the large particle size distribution due to the sensitivity of representative templates, such as micelles, to external factors [6] and complicated processes, and limited applications, due to the special materials, these methods are not recognized as practical solutions.

A carbon-based solution using polystyrene (PSt) particles, which contain abundant phenyl groups with a high carbonization efficiency, can be cited as a candidate for further study [14]. In polymer colloid chemistry, PSt is the most basic polymer you can use because of the ease of styrene polymerization [15-17], potential for formation of copolymers with various conjugated monomers [18], solubility in various solvents, and extensive previous research [19, 20]. Currently, a wide variety of non-spherical particles [21] such as hollow, porous, Janus, and golf ball-shaped particles can be produced without any template that needs to be removed [11, 22-26]. Nevertheless, little research has been done on maintaining the structure of PSt during carbonization due to its low thermal resistance [27, 28].

In this research, we developed a new method for the synthesis of PCHPs by carbonization of sub-micron hollow polymer particles, which retain their hollow structure due to hyper-cross-linking after thermal resistance treatment. This method is based on

particles made of styrene and divinylbenzene, the most versatile monomers and crosslinkers in polymer colloid chemistry, so it can be applied to the production of a wide variety of non-spherical particles. This research provides a simple and flexible method of synthesizing PCHPs for use in the sensor, catalysis, energy, and environmental industries.

2. Experimental

2.1 Materials

Unless otherwise noted, materials were used as received. Styrene (St), divinylbenzene (DVB), 2,2'-azobis[2-(2-imidazolin-2-yl)propane]dihydrochloride (VA-044) [15], toluene, 1,2-dichloroethane (DCE), and formaldehyde dimethyl acetal (FDA) were purchased from FUJIFILM Wako Pure Chemical Corporation. $FeCl_3$, HCl aqueous solution, and NaOH were bought from NACALAI TESQUE, INC. Poly-N-vinylacetamide (PNVA) was provided by Showa Denko K.K. as a 10 wt% aqueous solution. St was rinsed with 10 wt% $NaOH_{(aq)}$ and purified by vacuum distillation. Distilled water was produced by a distillation system (Auto Still WG250, Yamato).

2.2 Synthesis of seed particles (SPs)

SPs were synthesized by emulsion polymerization. St (1.8 g), $PNVA_{(aq)}$ (1.2 g), VA-044 (100 mg), and distilled water (120 mL) were added to a 200 mL batch reactor, and polymerization was carried out at 70 ℃, 130 rpm, for 18 h. SPs were collected by centrifugation. The average diameter of the SPs was 153 nm.

2.3 Synthesis of polymer hollow particles (PHPs)

PHPs were synthesized using the modified DSM [29]. The SPs (150 mg) were dispersed in ethanol, then St (1.6 g), DVB (0.4 g), toluene (0.28 g), and $PNVA_{(aq)}$ (0.5 g) were added to the PHPs colloid. Distilled water (50 mL) was added drop-wise into the colloid using a syringe pump at 3.6 mL/h with a stirring rate of 100rpm, then additional distilled water (50 mL) was added at 19.2 mL/h and the SPs grew with the addition of St, DVB, and toluene. VA-044 (10 mg) was then added, the temperature of the colloid was increased to 70 ℃, and the stirring rate was set to 130 rpm, causing surface polymerization to start. This time was defined as 0 h. After 2 h, additional VA-044 (10 mg) was added to the emulsion. The reaction continued for 8 h, then the PHPs were washed with water and ethanol twice each. The average diameter of PHPs was 344 nm, and the yield was 324 mg.

2.4 Hyper-cross-linking of PHPs

PHPs (54 mg) were dispersed in DCE (10 mL). FDA (1.14 g) and $FeCl_3$ (1.5 g) were added to the colloid, and Friedel-Crafts hyper-cross-linking started. For the first 3 h, the reaction proceeded at 40 °C, and the for the remaining 17 h the temperature was increased to 60 °C with a constant stirring rate of 100 rpm. The reaction was stopped by adding ethanol (8 mL) and 1 M HCl (2 mL). The particles were then washed with ethanol and water twice each. The hyper-cross-linked particles were named “HCL-PHPs”. The average diameter was 394 nm, and the yield was 78 mg.

2.5 Carbonization of HCL-PHPs

HCL-PHPs (78 mg) were placed in an alumina crucible. Carbonization was performed at a defined temperature between 700 and 900 °C in a nitrogen atmosphere for 3 h (heating rate: 5°C/min), after preheating in air to 320 °C, then 350 °C, for 15 min each (heating rate: 5 °C/min). The yields were 24.9 mg (700 °C), 23.8 mg (800 °C), and 17.3 mg (900 °C).

2.6 Characterization

The morphologies and sizes of the particles were determined by scanning electron microscopy (SEM, JSM-7500FA, JEOL). The hollow structures were observed by transmission electron microscopy (TEM, JEM-2100 plus, JEOL). The zeta potential of the SPs was measured by laser Doppler velocimetry (Zetasizer Nano-ZS, Malvern Panalytical, Ltd.). The Fourier Transform Infrared (FT-IR) spectrum method was obtained using attenuated total reflection (ATR) (FT/IR-4100, JASCO Corporation) with a diamond prism. The thermal resistance of the particles was measured by a thermal gravimetric analyzer (TGA, STA7200, Hitachi, Ltd.). The specific surface area and pore size distribution were measured by a nitrogen adsorption test using a BELSORP miniX (MicrotracBEL Corp.). The specific surface area was determined using the Brunauer-Emmett-Teller (BET) method. The pore size distribution was obtained by micropore (MP, for micropores) and Barrett-Joyner-Halenda analysis (BJH, for mesopores/micropores). The characteristics of the shells of the PCHPs were determined by Raman spectroscopy (NRS-1000, JASCO Corporation) and X-ray diffraction (XRD, Aeris research edition, Malvern Panalytical, Ltd.)

3. Results and discussion

In the modified DSM, PHPs were produced which consisted of poly(styrene-divinylbenzene) (Poly(St-DVB)) and were clearly hollow without any templates which

need to be removed (**Fig. 1**(a), (b)). SPs are positively charged due to the end groups of the initiator (zeta potential = 26.2 mV), and they disperse in ethanol with the aid of an added dispersant. Most of St, DVB, and toluene which were added to the colloid system were in the ethanol-rich disperse phase because they are miscible with ethanol.

As water was gradually added, the ratio of water to ethanol increased, and St, DVB, and toluene began to exhibit phase separation behavior because they could no longer remain dissolved in the disperse phase. Since they are all good solvents of PSt (solubility parameters: St: 8.7 $(cal/cm^3)^{0.5}$, DVB: 8.5 $(cal/cm^3)^{0.5}$ [30], toluene: 8.9 $(cal/cm^3)^{0.5}$[31], PSt: 8.7-9.1 $(cal/cm^3)^{0.5}$ [32]), some of them penetrate the SPs, causing them to swell instead of floating to the top of the dispersion medium [33]. After adding water, an emulsion that consists of polymers of SPs, St, DVB, and toluene was formed. After adding a water-soluble initiator to the emulsion, the water-soluble radicals were adsorbed and fixed to the surface of the emulsion because the surface had a high surface tension due to the end groups of the polymers forming SPs, and the polymerization of St and DVB proceeded near the surface [34, 35]. As polymerization proceeded, the St and DVB inside of the emulsion migrated to the surface, and a microgel of the crosslinked and solvent-insoluble P(St-DVB) became attached to the interface between the emulsion and the dispersed phase [23]. Furthermore, due to the polymerization shrinkage of the St and DVB [36, 37], PHPs composed of rigid shells and one clear void inside were synthesized. The surface of the PHPs was rough due to cross-linking by DVB [38].

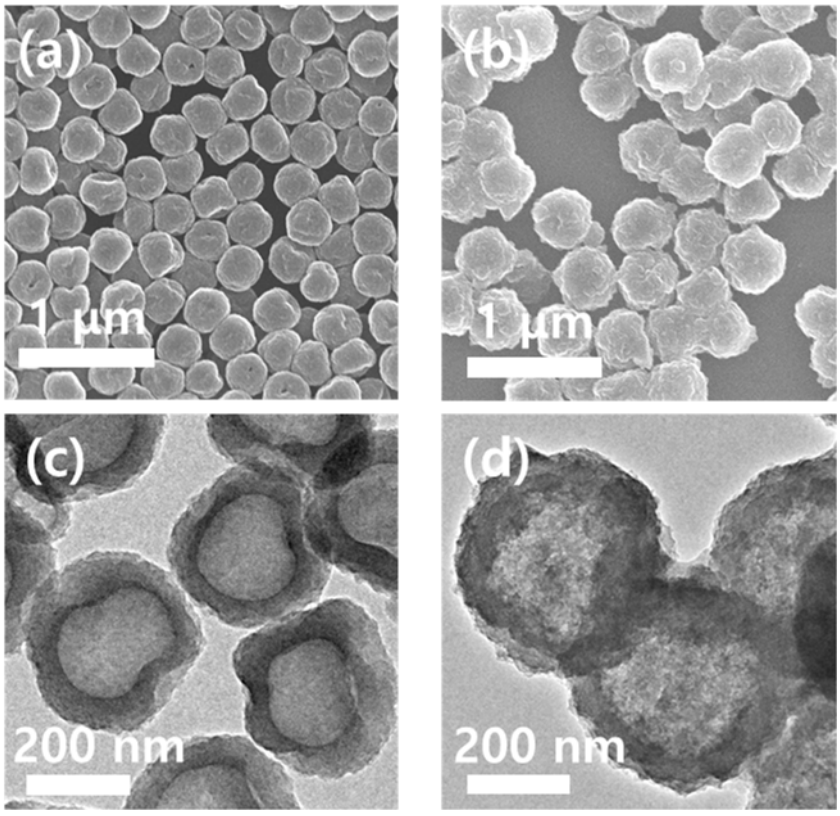

Fig. 1: SEM ((a), (b)) and TEM ((c), (d)) photographs of PHPs ((a), (c)) and HCL-PHPs ((b), (d)).

PHPs were cross-linked to some extent by DVB, however, additional hyper-cross-linking is necessary to achieve carbonization while maintaining their hollow structure. SEM and TEM photographs of HCL-PHPs are shown in **Fig. 1**(c) and (d). When the Friedel-Crafts alkylation reaction was applied to the PHPs, DCE and FDA acted as cross-linkers, and alkyl chains were inserted between the phenyl groups of the PHPs [39]. After the reaction, the color of the particles changed to light brown from white, and the diameter and weight of the HCL-PHPs increased to 115% and 144% compared to PHPs, respectively. In order to investigate the chemical structure changes caused by Friedel-Crafts alkylation more carefully, FT-IR analysis was performed on PHPs and HCL-PHPs (**Fig. 2**). Compared to PHPs, the absorption bands of HCL-PHPs at around 760 cm^{-1} and

695 cm^{-1} are weaker, which implies that the five adjacent Hs of the phenyl ring in Poly(St-DVB) are partly cross-linked [40]. Furthermore, TGA analysis in N_2 flow was executed to measure the thermal resistance of PHPs and HCL-PHPs (**Fig. 3**). Weight losses at 700 °C were 94.5% (PHPs) and 72.7% (HCL-PHPs), this result clearly shows that Friedel-Crafts alkylation successfully improves the thermal resistance of PHPs.

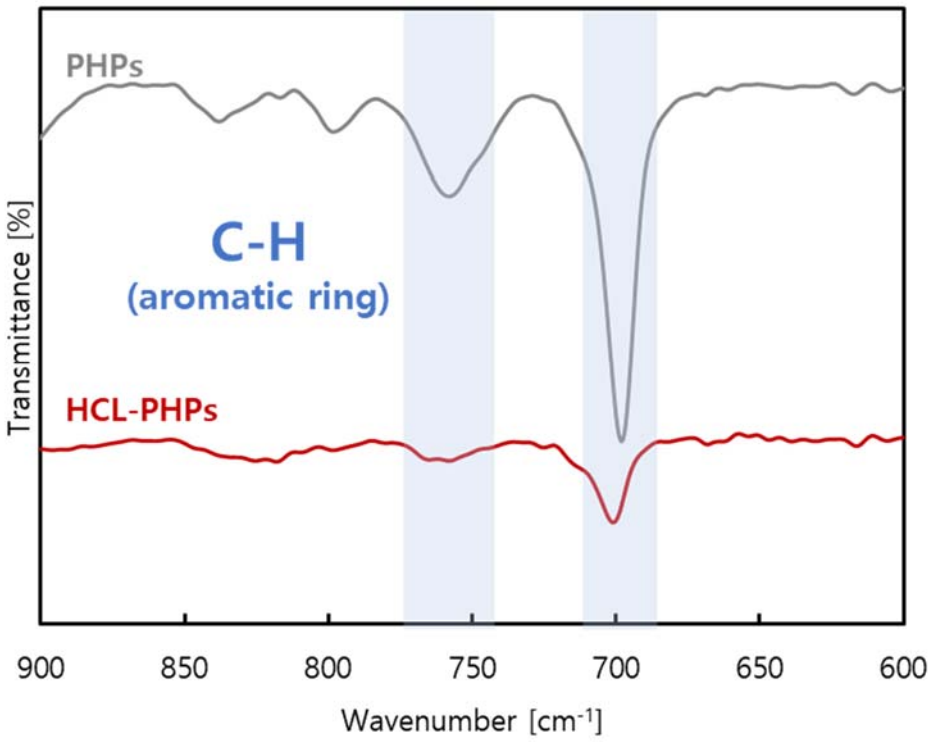

Fig. 2: FT-IR spectra for PHPs and HCL-PHPs.

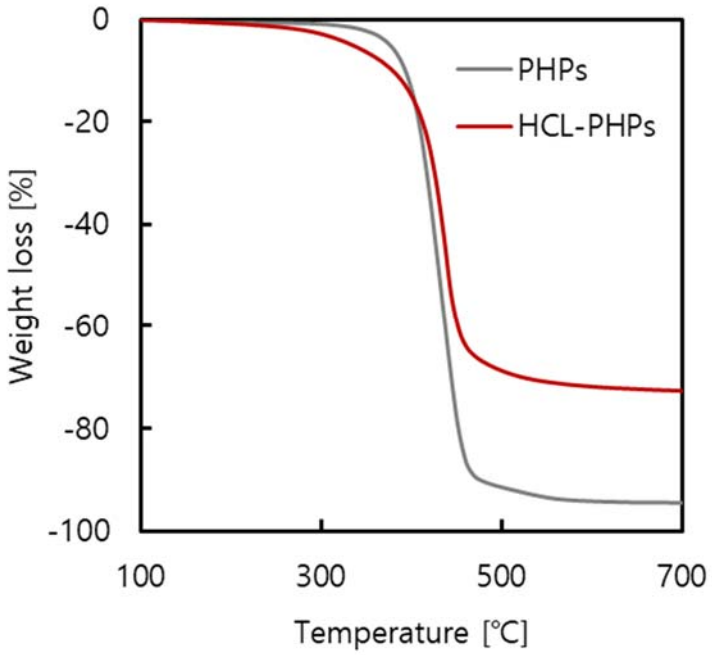

Fig. 3: TGA curves for PHPs and HCL-PHPs measured in nitrogen flow.

The hyper-cross-linking reaction effectively improves the thermal resistance of PHPs, and PCHPs obtained by the carbonization at high temperature of HCL-PHPs retain their hollow structures (**Fig. 4**). Outer particle diameter (D_p), inner particle diameter (hollow section) (D_h), specific surface area determined by BET (S_{BET}), and peak intensity ratio between the G and D bands (I_G/I_D) are summarized in **Table 1**. Regardless of the carbonization temperature, the particle size of PCHPs decreased from that of HCL-PHPs because of the framework shrinkage due to mass loss after carbonization [41]. When the carbonization temperature was 700 °C, shell collapse was hardly observed, meanwhile at 800 °C the hollow structure was maintained though some visible pores were observed. On the other hand, at 900 °C, many shells collapsed and their insides were exposed.

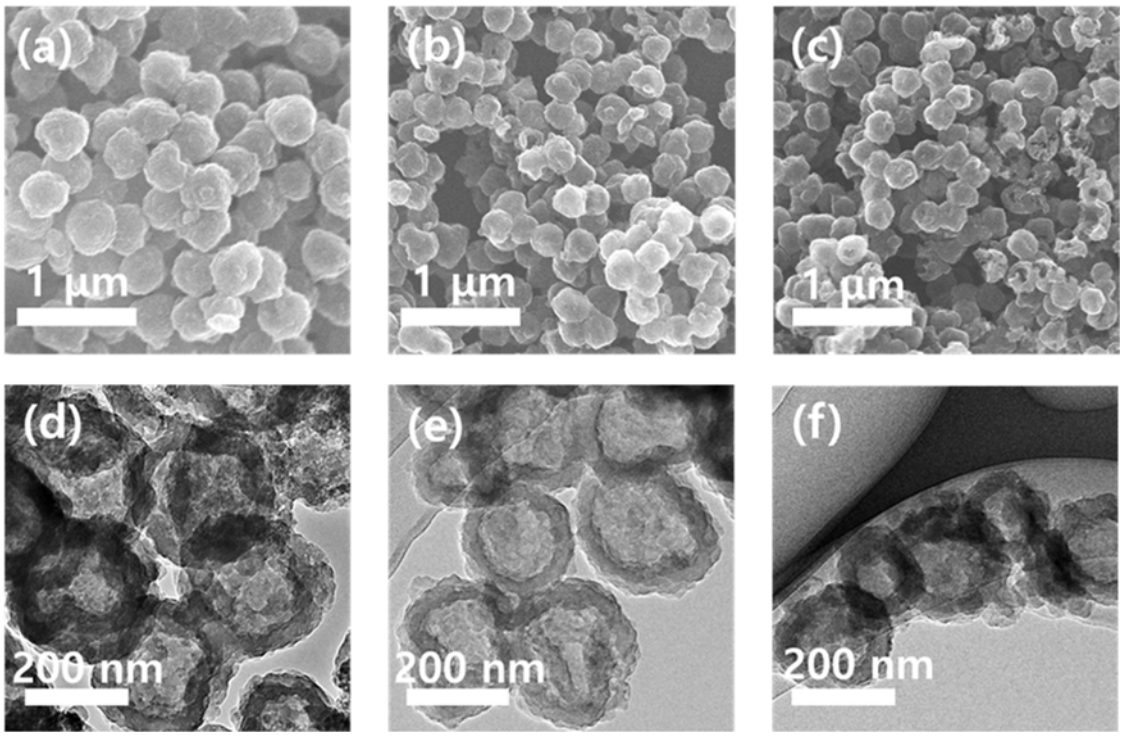

Fig. 4: SEM ((a)~(c)) and TEM ((d)~(f)) photographs of PCHPs. Carbonization temperatures are 700 °C ((a), (d)), 800 °C ((b), (e)), and 900 °C ((c), (f)).

Table. 1. Outer particle diameter (D_p), inner particle diameter (hollow section) (D_h), specific surface area determined by BET (S_{BET}), and peak intensity ratio between the G and D bands (I_G/I_D).

Carbonization temperature [°C]	D_p [nm]	D_h [nm]	S_{BET} [m^2/g]	I_G/I_D [-]
700	267	170	658	1.20
800	263	160	805	1.01
900	258	120	945	0.92

Nitrogen adsorption and desorption tests of PCHPs showed that they possessed abundant micropores and hollow-derived micropores (**Fig. 5**). All the samples had large BET specific surface areas, and these increased as the carbonization temperature rose.

Regardless of the carbonization temperature, the adsorption and desorption isotherms of nitrogen feature the characteristics of the I / IV type based on IUPAC categories (**Fig. 5**(a)). The increase in the adsorption isotherm at low relative pressures indicates the presence of abundant micropores in PCHPs due to the dense polymer network from hyper-cross-linking [42] or the presence of numerous defects in the carbon shell [43]. The micropore size distribution obtained by MP analysis (**Fig. 5**(b)) represents that the shell contains very narrow pores (about 0.6 nm). The rise of the adsorption isotherm at high pressures and the clear hysteresis loop indicates the presence of meso-macropores derived from the hollow structure [44]. Although the pore size distribution obtained by BJH analysis (**Fig. 5**(c)) indicated the possibility of the space among the particles, the peak was found at almost the same radius as the hollow radius measured by TEM and supported the existence of hollow in the particle. Therefore, it was shown that CHPs synthesized by this method clearly have a hollow structure inside the porous carbon shell.

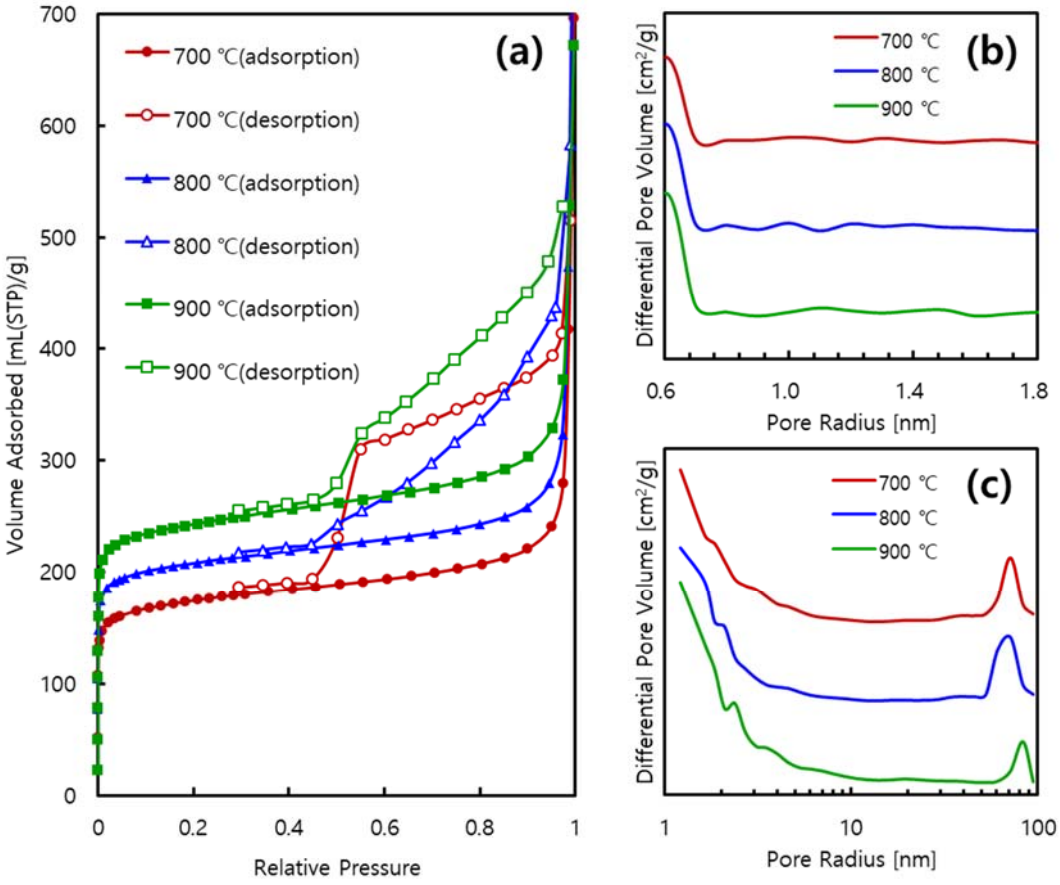

Fig. 5: (a): Adsorption and desorption isotherm, (b): micro pore distribution by MP analysis, (c): meso/macro pore distribution by BJH analysis of PCHPs. The temperatures listed in the legend indicate the carbonization temperature.

Raman spectroscopy and XRD measurements clearly show that PCHPs are composed of partly graphite-structured amorphous carbon (**Fig. 6, 7**). In the Raman spectrums of CHPs (**Fig. 6**), the peak at about 1580 cm^{-1} (G band) corresponds to the E_{2g} mode of hexagonal graphite and relates to the vibration of sp^2-bonded carbon atoms in graphite layers. The peak at approximately 1350 cm^{-1} shows that the vibration of carbon atoms with dangling bonds is in the termination plane of disordered graphite [28]. As information about aromatic rings is incorporated in the peak intensity, not peak area [45], the I_G/I_D ratio was measured using the maximum band intensity. The small I_G/I_D ratio indicates that the carbon shells of CHPs contain many defects [43]. The XRD pattern (**Fig.**

7) shows the characteristics of amorphous carbon partially crystallized to a graphite structure. The broad and intense spectrum at low angles indicates the presence of dense pores [46]. The gentle peak around 23° shows diffraction from the (002) plane of the disordered amorphous carbon graphite structure [47]. The clear peaks from 25.5° to 26° show diffraction from the (002) plane of the highly crystallized graphite structure [48]. The inter-surface distance of this section is 0.358 nm, which is similar to that of graphite (0.335 nm [49]). The peaks from 42° to 44° indicate a plane of amorphous carbon (100), suggesting a mild graphite structure due to the occurrence of carbon intercalation [50]. This peak appears to have a sharp peak on top of a gentle peak, indicating that both dense and coarse graphite structures exist in the shells. Although it is small, a peak from the (004) plane near 53°, which shows a more highly crystalline graphite structure, was also observed [51]. The peaks around 35° correspond to the (110) plane of α-Fe_2O_3 or the (311) plane of face-centered Fe_3O_4 which is derived from left-over $FeCl_3$ catalyst [52].

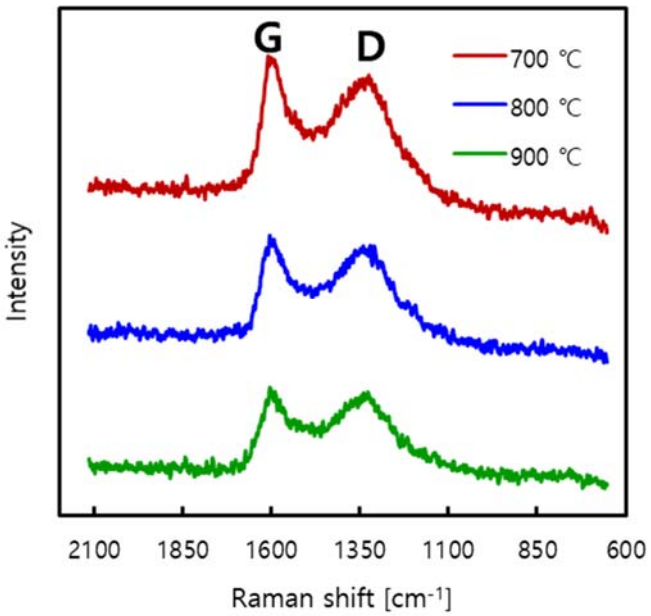

Fig. 6: Raman shifts of PCHPs. The temperatures listed in the legend indicate the carbonization temperatures.

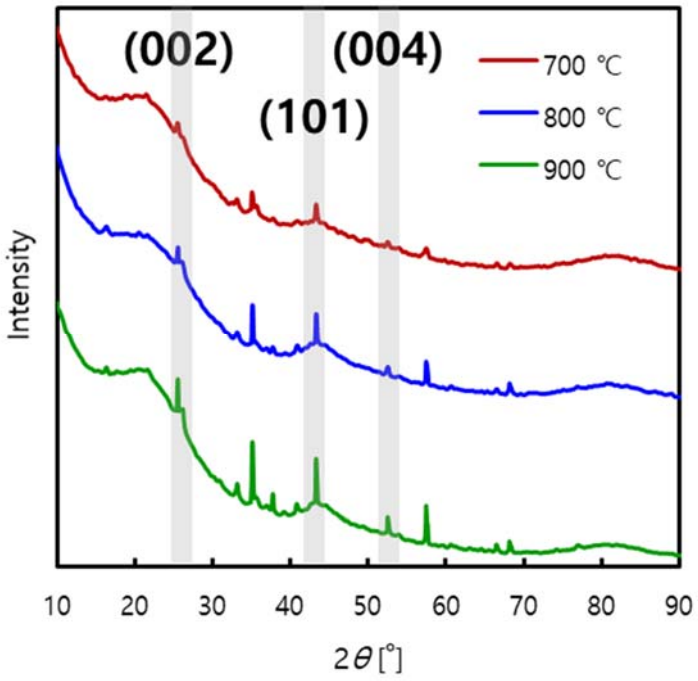

Fig. 7: XRD patterns of PCHPs. The temperatures listed in the legend indicate the carbonization temperatures.

4. Conclusion

We successfully synthesized PCHPs by modified DSM without using templates which need to be removed before use of PHPs as a raw material. The Friedel-Crafts alkylation inserted a hyper-cross-linked structure of alkyl chains between the phenyl groups of PHPs, which improved their heat resistance. PCHPs retained their hollow structure after carbonization by heating in air. PCHPs had abundant mesopores and void-derived macropores, and their shells were composed of amorphous carbon. This simple and versatile method provides new value in for use in the sensor, catalysis, and energy, and environmental industries.

Acknowledgment

The authors are grateful to Prof. Tanabe and Dr. Irisawa in Nagoya University for insightful comments and suggestions. The XRD measurements were supported by Prof. Takami and Mr. Nohara in Nagoya University. This study was financially supported in part by Scientific Research (B) from the Ministry of Education, Culture, Sports, Science and Technology of Japan, (No. 18H01777).

References

[1] G. Wang, R. Wang, L. Liu, H. Zhang, J. Du, Y. Zhang, M. Liu, K. Liang, A. Chen, Synthesis of hollow mesoporous carbon spheres via Friedel-Crafts reaction strategy for supercapacitor, Materials Letters, 197 (2017) 71-74.
[2] X. Liu, J. Wu, S. Zhang, C. Ding, G. Sheng, A. Alsaedi, T. Hayat, J. Li, Y. Song, Amidoxime-Functionalized Hollow Carbon Spheres for Efficient Removal of Uranium from Wastewater, ACS Sustainable Chemistry & Engineering, 7 (2019) 10800-10807.
[3] J. Liu, N.P. Wickramaratne, S.Z. Qiao, M. Jaroniec, Molecular-based design and emerging applications of nanoporous carbon spheres, Nat Mater, 14 (2015) 763-774.
[4] H. Xu, X. Yin, M. Zhu, M. Han, Z. Hou, X. Li, L. Zhang, L. Cheng, Carbon Hollow Microspheres with a Designable Mesoporous Shell for High-Performance Electromagnetic Wave Absorption, ACS Appl Mater Interfaces, 9 (2017) 6332-6341.
[5] S. Choudhury, T. Ebert, T. Windberg, A. Seifert, M. Göbel, F. Simon, P. Formanek, M. Stamm, S. Spange, L. Ionov, Hierarchical Porous Carbon Cathode for Lithium–Sulfur Batteries Using Carbon Derived from Hybrid Materials Synthesized by Twin Polymerization, Particle & Particle Systems Characterization, 35 (2018).
[6] S. Li, A. Pasc, V. Fierro, A. Celzard, Hollow carbon spheres, synthesis and applications – a review, Journal of Materials Chemistry A, 4 (2016) 12686-12713.
[7] D. Liu, L.T. Tufa, J. Lee, N-doped microporous carbon hollow spheres with precisely controlled architectures for supercapacitor, Electrochimica Acta, 313 (2019) 389-396.
[8] X. Lai, J.E. Halpert, D. Wang, Recent advances in micro-/nano-structured hollow spheres for energy applications: From simple to complex systems, Energy Environ. Sci., 5 (2012) 5604-5618.
[9] L. Chuenchom, R. Kraehnert, B.M. Smarsly, Recent progress in soft-templating of porous carbon materials, Soft Matter, 8 (2012).
[10] L. Zhou, Z. Zhuang, H. Zhao, M. Lin, D. Zhao, L. Mai, Intricate Hollow Structures: Controlled Synthesis and Applications in Energy Storage and Conversion, Adv Mater, 29 (2017).
[11] R.A. Ramli, Hollow polymer particles: a review, RSC Advances, 7 (2017) 52632-

52650.
[12] Z. He, M. Zhou, T. Wang, Y. Xu, W. Yu, B. Shi, K. Huang, Hyper-Cross-Linking Mediated Self-Assembly Strategy To Synthesize Hollow Microporous Organic Nanospheres, ACS Appl Mater Interfaces, 9 (2017) 35209-35217.
[13] S. Kandambeth, V. Venkatesh, D.B. Shinde, S. Kumari, A. Halder, S. Verma, R. Banerjee, Self-templated chemically stable hollow spherical covalent organic framework, Nat Commun, 6 (2015) 6786.
[14] C.H. Kim, D.-K. Lee, T.J. Pinnavaia, Graphitic Mesostructured Carbon Prepared from Aromatic Precursors, Langmuir, 20 (2004) 5157-5159.
[15] T. Yamamoto, T. Yokoyama, Effect of Counter Ionic Radius in Initiator on Particle Size in Soap-free Emulsion Polymerization of Styrene, Chemistry Letters, 44 (2015) 824-825.
[16] T. Yamamoto, K. Kawaguchi, Effect of electrolyte species on size of particle through soap-free emulsion polymerization of styrene using AIBN and electrolyte, Colloid Polym Sci, 293 (2015) 1003-1006.
[17] T. Yamamoto, Y. Kanda, K. Higashitani, Initial growth process of polystyrene particle investigated by AFM, Journal of colloid and interface science, 299 (2006) 493-496.
[18] T. Yamamoto, K. Kawaguchi, Relationship between surface potential and particle size in soap-free emulsion copolymerization of styrene and methyl methacrylate using a water- or oil-soluble initiator, Colloid Polym Sci, 294 (2015) 281-284.
[19] V. Chaudhary, S. Sharma, Suspension polymerization technique: parameters affecting polymer properties and application in oxidation reactions, Journal of Polymer Research, 26 (2019).
[20] B. Yu, H. Cong, Q. Peng, C. Gu, Q. Tang, X. Xu, C. Tian, F. Zhai, Current status and future developments in preparation and application of nonspherical polymer particles, Adv Colloid Interface Sci, 256 (2018) 126-151.
[21] Y. Kawai, T. Yamamoto, Synthesis of dimpled and submicron-sized polymer particles of different morphologies using free micromixer, Colloid and Interface Science Communications, 32 (2019).
[22] C. Huang, H. Kobayashi, M. Moritaka, M. Okubo, Hollow particles are produced by the burying of sulfate end-groups inside particles prepared by emulsion polymerization of styrene with potassium persulfate as initiator in the absence/presence of a nonionic emulsifier, Polymer Chemistry, 8 (2017) 6972-6980.
[23] S. Nuasaen, P. Tangboriboonrat, Highly charged hollow latex particles prepared via seeded emulsion polymerization, J Colloid Interface Sci, 396 (2013) 75-82.
[24] R. Yan, Y. Zhang, X. Wang, J. Xu, D. Wang, W. Zhang, Synthesis of porous poly(styrene-co-acrylic acid) microspheres through one-step soap-free emulsion polymerization: whys and wherefores, J Colloid Interface Sci, 368 (2012) 220-225.
[25] N. Yamashita, N. Konishi, T. Tanaka, M. Okubo, Preparation of hemispherical polymer particles by cleavage of a Janus poly(methyl methacrylate)/polystyrene composite particle, Langmuir, 28 (2012) 12886-12892.
[26] H. Huang, H. Liu, Synthesis of the raspberry-like PS/PAN particles with anisotropic properties via seeded emulsion polymerization initiated by γ-ray radiation, Journal of Polymer Science Part A: Polymer Chemistry, 48 (2010) 5198-5205.
[27] H. Lu, C.A. Wilkie, Synergistic effect of carbon nanotubes and decabromodiphenyl oxide/Sb2O3 in improving the flame retardancy of polystyrene, Polymer Degradation and

Stability, 95 (2010) 564-571.
[28] J. Gong, J. Liu, X. Chen, X. Wen, Z. Jiang, E. Mijowska, Y. Wang, T. Tang, Synthesis, characterization and growth mechanism of mesoporous hollow carbon nanospheres by catalytic carbonization of polystyrene, Microporous and Mesoporous Materials, 176 (2013) 31-40.
[29] M. Okubo, H. Minami, Formation mechanism of micron-sized monodispersed polymer particles having a hollow structure, Colloid & Polymer Science, 275 (1997) 992-997.
[30] Y. Cai, W. Yan, X. Peng, M. Liang, L. Yu, H. Zou, Influence of solubility parameter difference between monomer and porogen on structures of poly (acrylonitrile-styrene-divinylbenzene) resins, Journal of Applied Polymer Science, 136 (2019).
[31] G. Hu, D. Yu, J. Zhang, H. Liang, Z. Cao, Synthesis of micron-sized poly(styrene-co-divinylbenzene) hollow particles from seeded emulsions by using swelling solvents, Colloid Journal, 73 (2011) 557-564.
[32] Y. Li, J. Chen, A. Niu, F. Xue, Y. Cao, Q. Xu, Preparation of hollow poly (styrene-co-divinylbenzene) particles with variable cavity sizes and further fabrication of hollow TiO2 particles using solid poly (styrene-co-divinylbenzene) particles as templates, Colloids and Surfaces A: Physicochemical and Engineering Aspects, 342 (2009) 107-114.
[33] M. Okubo, M. Shiozaki, M. Tsujihiro, Y. Tsukuda, Preparation of micron-size monodisperse polymer particles by seeded polymerization utilizing the dynamic monomer swelling method, Colloid & Polymer Science, 269 (1991) 222-226.
[34] C.J. McDonald, K.J. Bouck, A.B. Chaput, C.J. Stevens, Emulsion Polymerization of Voided Particles by Encapsulation of a Nonsolvent, Macromolecules, 33 (2000) 1593-1605.
[35] H. Lv, Q. Lin, K. Zhang, K. Yu, T. Yao, X. Zhang, J. Zhang, B. Yang, Facile fabrication of monodisperse polymer hollow spheres, Langmuir, 24 (2008) 13736-13741.
[36] N. Itou, T. Masukawa, I. Ozaki, M. Hattori, K. Kasai, Cross-linked hollow polymer particles by emulsion polymerization, Colloids and Surfaces A: Physicochemical and Engineering Aspects, 153 (1999) 311-316.
[37] T. Yamamoto, S. Kim, Anomalous particle through soap-free emulsion polymerization of styrene using oil-soluble initiator, J Polym Res, 24 (2017).
[38] M.D.G. de Luna, M.F. Divinagracia, A.E.S. Choi, D.C. Ong, T.-W. Chung, Applicability of Composite Silica–Divinylbenzene in Bioethanol Dehydration: Equilibrium, Kinetic, Thermodynamic, and Regeneration Analysis, Energy & Fuels, 33 (2019) 7347-7356.
[39] A. Hu, W. Zhang, Q. You, B. Men, G. Liao, D. Wang, A green and low-cost strategy to synthesis of tunable pore sizes porous organic polymers derived from waste-expanded polystyrene for highly efficient removal of organic contaminants, Chemical Engineering Journal, 370 (2019) 251-261.
[40] Z. Fu, J. Jia, J. Li, C. Liu, Transforming waste expanded polystyrene foam into hyper-crosslinked polymers for carbon dioxide capture and separation, Chemical Engineering Journal, 323 (2017) 557-564.
[41] K. Wang, L. Huang, S. Razzaque, S. Jin, B. Tan, Fabrication of Hollow Microporous Carbon Spheres from Hyper-Crosslinked Microporous Polymers, Small, 12 (2016) 3134-3142.
[42] Y. Ouyang, H. Shi, R. Fu, D. Wu, Highly monodisperse microporous polymeric and carbonaceous nanospheres with multifunctional properties, Sci Rep, 3 (2013) 1430.

[43] F. Xu, Z. Tang, S. Huang, L. Chen, Y. Liang, W. Mai, H. Zhong, R. Fu, D. Wu, Facile synthesis of ultrahigh-surface-area hollow carbon nanospheres for enhanced adsorption and energy storage, Nat Commun, 6 (2015) 7221.
[44] M. Šoltys, M. Balouch, O. Kašpar, M. Lhotka, P. Ulbrich, A. Zadražil, P. Kovačík, F. Štěpánek, Evaluation of scale-up strategies for the batch synthesis of dense and hollow mesoporous silica microspheres, Chemical Engineering Journal, 334 (2018) 1135-1147.
[45] T. Schott, J.L. Gómez-Cámer, P. Novák, S. Trabesinger, Relationship between the Properties and Cycle Life of Si/C Composites as Performance-Enhancing Additives to Graphite Electrodes for Li-Ion Batteries, Journal of The Electrochemical Society, 164 (2016) A190-A203.
[46] Y. Zhu, S. Murali, M.D. Stoller, K.J. Ganesh, W. Cai, P.J. Ferreira, A. Pirkle, R.M. Wallace, K.A. Cychosz, M. Thommes, D. Su, E.A. Stach, R.S. Ruoff, Carbon-based supercapacitors produced by activation of graphene, Science, 332 (2011) 1537-1541.
[47] Q. Wang, X. Liang, W. Qiao, C. Liu, X. Liu, L. Zhan, L. Ling, Preparation of polystyrene-based activated carbon spheres with high surface area and their adsorption to dibenzothiophene, Fuel Processing Technology, 90 (2009) 381-387.
[48] B. Xu, H. Duan, M. Chu, G. Cao, Y. Yang, Facile synthesis of nitrogen-doped porous carbon for supercapacitors, Journal of Materials Chemistry A, 1 (2013).
[49] M. Pawlyta, J.-N. Rouzaud, S. Duber, Raman microspectroscopy characterization of carbon blacks: Spectral analysis and structural information, Carbon, 84 (2015) 479-490.
[50] B. Hu, L.-B. Kong, L. Kang, K. Yan, T. Zhang, K. Li, Y.-C. Luo, Synthesis of a hierarchical nanoporous carbon material with controllable pore size and effective surface area for high-performance electrochemical capacitors, RSC Advances, 7 (2017) 14516-14527.
[51] Y. Xia, R. Mokaya, Synthesis of Ordered Mesoporous Carbon and Nitrogen-Doped Carbon Materials with Graphitic Pore Walls via a Simple Chemical Vapor Deposition Method, Advanced Materials, 16 (2004) 1553-1558.
[52] W.-M. Zhang, X.-L. Wu, J.-S. Hu, Y.-G. Guo, L.-J. Wan, Carbon Coated Fe3O4Nanospindles as a Superior Anode Material for Lithium-Ion Batteries, Advanced Functional Materials, 18 (2008) 3941-3946.